Proceedings of the Canadian Society for Mechanical Engineering International Congress
32nd Annual Conference of the Computational Fluid Dynamics Society of Canada
Canadian Society of Rheology Symposium
CSME-CFDSC-CSR 2025
May 25–28, 2025, Montréal, Québec, Canada

Impact Analysis on Non-Planar 3D-Printed FFF Parts

Felipe M. Franco, Aleksander Czekanski*
Lassonde School of Engineering, York University, Toronto, Canada
*alex.czekanski@lassonde.yorku.ca

Abstract—This study investigates the Charpy impact resistance of non-planar 3D-printed parts manufactured by fused filament fabrication (FFF). Traditional planar slicing introduces anisotropy and layer delamination, leading to suboptimal mechanical properties. Non-planar slicing methods, such as sinusoidal and bell-shaped patterns, offer promising enhancements by optimizing layer alignment and stress distribution. Five sample variations were designed using FullControl GCode Designer and tested following ASTM D6110 standards. Results indicate a significant improvement in impact strength for vertically oriented non-planar specimens, with up to 50% greater resistance than planar counterparts, as well as reduced anisotropy when comparing horizontally and vertically fabricated parts. This work highlights the potential of non-planar slicing for reducing anisotropy and improving the structural integrity of FFF parts, offering insights for industrial applications requiring tougher 3D-printed components.

Keywords – 3D printing; Charpy impact; non-planar printing; fracture.

I. INTRODUCTION

3D-printing FFF is a fabrication method that deposits plastic filaments in a surface to build a part in incremental steps. These steps, called layers, must be fabricated sequentially, one over the other, to manufacture the final 3D-printed object. The creation of these layers consists of a process called slicing, in which the object is discretized in segments, usually by equidistant planes parallel to the machine's print bed, in a technique known as "planar slicing". Although planar slicing is the most straightforward form of creating the layers, it has inherent weaknesses, such as anisotropy and delamination [1].

A. Non-Planar Printing

First conceived theoretically by Chakraborty et al. [2], non-planar slicing removes the limitation of having strictly planar layers to divide the 3D object. It is an opportunity to use anisotropy in our favour and enable numerous optimization possibilities, from physical properties to the appearance and smoothness of the constructs. It also provides the tools to implement a continuous and highly customizable filament deposition throughout the layer [3][4].

These property enhancements can be based on empirical observations or scientific analysis. Some studies [5][6] employed FEA analysis to optimize toolpaths and improve part manufacturing for specific known loads in single-use cases. However, broader and more generalized approaches can also yield improvements. For instance, earlier research compared planar-sliced parts with samples featuring layers aligned to their exterior geometry [7][8][9]. Others examined the effects of incorporating common patterns into the Z-axis toolpath [10][11], regarded as the weakest direction in planar prints.

Unfortunately, assembling the non-planar toolpaths is not a trivial process, and this option is still unavailable in commercial, widely used slicers. Several mathematical and vectorial techniques were developed over the years to tackle this issue [5][12][13], though they were not made public for general use. An outlier in this regard is FullControl GCode Designer [14], a VBA-based Excel tool that generates machine instructions based on input parameters and formulas. This low-level GCode management is essential to control the toolpath and create the non-planar layers from scratch. Though not technically a "slicing" technique, as it does not segment a source geometry and asks the user to control the printhead manually, it can be programmed to recreate the same physical results.

B. Impact Testing

Mechanical testing is a standardized way to assess the properties of materials and parts. They are of utmost importance in mechanical engineering, helping to design more suitable parts for all applications. One of them is impact testing, which measures the resistance of a specimen against a sudden high-energy flexural shock. Among many options, the Charpy Impact Test is an experiment broadly employed to evaluate impact strength. It accelerates a pendulum towards a specimen and measures the energy consumed by the pendulum to break the specimen, including crack initiation and propagation, creation of new surfaces and overall losses due to friction and vibration (measured beforehand and compensated for after the test). In

addition, a center notch aligned to the impact plane is made on the sample to induce controlled crack initiation [16].

Previous work regarding impact testing in non-planar 3D printed parts is rare. Allum et al. [10] created thin-walled parts using FullControl GCode Designer but tested them only in tension, while Kayali et al. [15] focused on the microstructure of the parts designed with the same software. Digging up Charpy Impact testing results on planar-sliced PLA 3D-printed parts with 100% infill, on the other hand, was more common. Results ranged from 2.5 to 25.9 kJ/m^2 depending on printing orientation. Table I brings the published measurements, but since most of these studies focused on material reinforcements of PLA, only the baseline values were included. This paper aims to use 3D-printed samples composed of varied non-planar layer patterns using FullControl GCode Designer and evaluate their impact resistance using the Charpy method described in ASTM D6110, helping to fill this gap in the current literature.

II. METHOD

Five variations of the Charpy sample were designed for this study: Planar Horizontal (PH), Planar Vertical (PV), Sinusoidal Horizontal (SH), Sinusoidal Vertical (SV) and Bell-shaped (Figure 1). All samples were set to have their material deposited either at 0 or 90 degrees with respect to the axis of the Charpy impact. The sinusoidal or bell-shaped variations for the non-planar specimens were designed to occur in the printing direction to investigate the layer adhesion upon sudden stress. These toolpaths were created in FullControl GCode Designer with the parameters present in Table II.

The sinusoidal shape was implemented to try and distribute the stresses imposed on the sample along its deposited filaments. In planar specimens, all layers are either perpendicular or parallel to the impact, whereas in the sinusoidal slicings, the angles vary continuously between ± 45º. This shift means that the impact stress will travel both between and through the layers, depending on the angle of the region. In the SV and SH samples, the frequency and amplitude were chosen to result in an entire number of waves while maximizing the deposition angle that the stock nozzle of the printer could achieve. In this study, this angle is 45° for a regular Prusa Nextruder nozzle on a 3-DoF (degree of freedom) printer. The waves were phased 90° from their original starting point to improve printability, as each layer would start from the bottom of the wave, connecting with the material previously deposited. As for the Bell samples, they were designed as a compromise between the slicings. The non-planar variation was placed on the impact plane, with a design that resembles a half-sinewave. This shape was chosen to reinforce the stress path present on the Charpy test [26], mimicking a slicing variation that would be optimized using FEA analysis for this use. Apart from this region, towards the edges of the Bell specimen, the deposition was identical to the planar samples. Compensation layers were designed to complete the shape as the end geometry required a perfect parallelepiped for notching.

All samples were printed in a Prusa™ Mk4 [Prusa Research, Czech Republic], a 3-DoF, enclosed machine. Five units of each sample were made using Polymaker's Polyterra™ PLA material [Polymaker, China] to the parameters in Table III. All the samples were finished using pliers and sandpaper, weighed, measured to assure compliance with the standard geometry, and notched before the experiment.

The impact test was run to ASTM D6110 standards. The Charpy impact test was performed in an Instron™ CP9050 machine [Instron Corp., United States of America]. The calibration of the machine and the assessment of the energy lost due to pendulum movement and friction were made before each batch of tests. Post-failure images were obtained after failure in a ZEISS Axio Imager 2 optical microscope with an Axiocam 506 color/mono module [Carl Zeiss AG, Germany].

TABLE I. LITERATURE MEASUREMENTS OF IMPACT RESISTANCE FOR PLA SAMPLES

Study	Year	Impact Resistance (kJ/m^2)	Printing Orientation x Charpy Impact
Tanveer et al. [17]	2019	4.75	Perpendicular
Fekete et al. [18]	2021	15.5	Perpendicular
Andrzejewski et al. [19]	2022	2.5	45 degrees
Shaik et al. [20]	2023	14.2	Perpendicular
		12.7	Parallel
Muthe et al. [21]	2024	20.9	Perpendicular
Shang et al. [22]	2024	25.9	Perpendicular
Murariu et al. [23]	2024	3.7	45 degrees
Głowacki et al. [24]	2024	19	45 degrees

TABLE II. DESIGNING PARAMETERS FOR THE NON-PLANAR SAMPLES

Sample	Max. Amplitude (mm)	Frequency
SV	± 0.508	2
SH	± 1	10
Bell	-2	1

TABLE III. PRINTING PARAMETERS FOR ALL SAMPLES

Parameter	Value
Nozzle Temperature (°C)	220
Bed Temperature (°C)	60
Velocity (mm/s)	30
Infill (%)	100
Layer Height (mm)	0.2

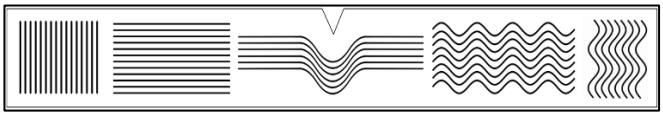

Figure 1. Graphical representations of the slicing techniques used in this experiment superimposed in the Charpy sample, from left to right: PV, PH, Bell, SH and SV

III. RESULTS

TABLE IV. IMPACT TEST RESULTS FOR ALL SAMPLES

Sample	Average Impact Strength (kJ/m^2)	Non-Planar Enhancement	Anisotropy
PV	1.368 ± 0.078	Ref. SV	Ref. PH.
SV	2.060 ± 0.427	50.60%	Ref. SH.
PH	4.775 ± 0.150	Ref. SH, Bell	249.00%
SH	4.810 ± 0.279	0.70%	133.50%
Bell	5.022 ± 0.580	5.20%	-

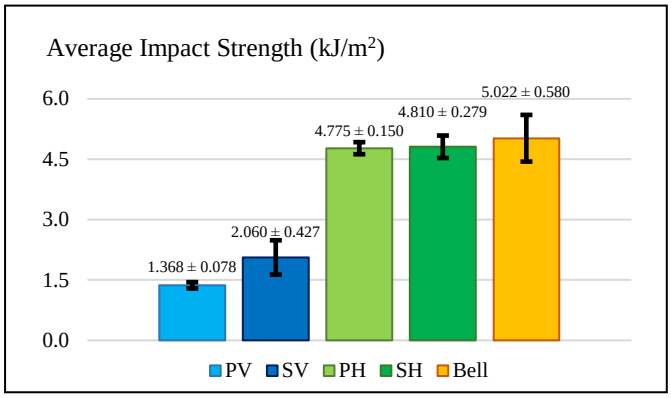

Figure 2. Comparison chart with the average impact strength for all samples

Figure 3. PV (top left) and SV (bottom left) samples and comparison (right)

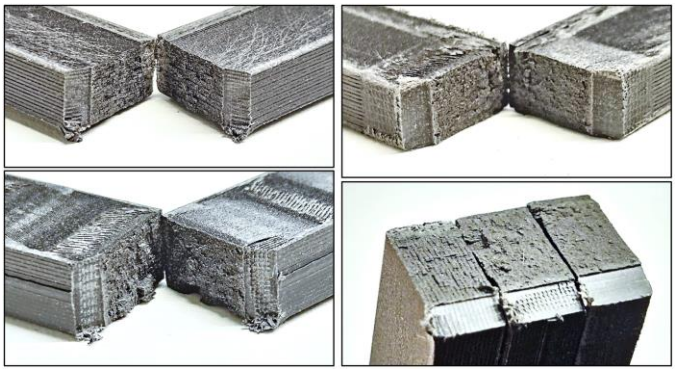

Figure 4. PH (top left), SH (bottom left) and Bell (top right) samples and comparison (bottom right, same order) after testing

A. *Impact Strength*

Table IV and Figure 2 show the results for the energy required to break each sample testes. The average impact strength for the vertical samples was 1.368 ± 0.078 kJ/m^2 on the planar-printed part and 2.060 ± 0.427 kJ/m^2 for the sinusoidal part, a statistically significant improvement of 50.6% ($p = 0.021$). For the horizontal models, the planar sample required 4.775 ± 0.150 kJ/m^2 to break, compared to 4.810 ± 0.279 kJ/m^2 for the sinusoidal counterpart ($p = 0.813$) and 5.022 ± 0.580 kJ/m^2 for the Bell sample ($p = 0.403$), both of which cannot be considered statistically different from the planar reference. These results fit the lower end of the range presented in Table 1, agreeing with previous literature on impact testing on PLA. As for comparing the anisotropy of the planar pair and the non-planar pair, the sinusoidal slicing helped to reduce the performance difference from 249% to 133.5%, reducing the orientation dependence of the models.

B. *Fracture Profile*

Both vertical specimens had a similar fracture profile: a progression of the crack in the interlayer surface to break the specimen. The planar-layered PV was the weakest in withstanding impact and showed a very flat and smooth fracture, characteristic of brittle materials (Figure 3). The fracture surface is very clean, and most samples exhibited perfect delamination, resulting in a piece that could be mistaken for a half-printed part (Figure 5A). The non-planar specimen also showed delamination, but along the curved layer profile, which suggests that the crack path was lengthier and tougher than the one on the PV sample (Figure 5B). The fracture surface also appears rougher, and more individual filaments on the SV sample appear to have been torn apart compared to PV. The parts manufactured horizontally presented very similar behaviours in performance and fracture profile. All samples presented a straightforward rupture of the PLA strands on the impact plane (Figures 4, 5C, 5E and 5G).

Microscopy on the fracture surface revealed that the PH sample presented more voids on its meso-structure (Figure 5D) than the SH and Bell samples in the plane of impact (Figures 5F and 5H, respectively). The aligned voids (purple arrows) on the planar-sliced part create a defined and linear pathway for the crack propagation, contributing to the slightly lower impact resistance measured. The non-planar samples, in turn, show voidless regions (yellow outlines) that better resist the impact energy and randomly located grouped voids (purple arrows) that make the crack path tortuous and tougher to cut across.

IV. DISCUSSION

The average impact resistance of the SV sample surpassed that of the PV sample by 50%, showing great reinforcement of the material when hit perpendicularly to its layers. As the layers on the SV sample are curved, it takes more physical distance along the layer boundary for the crack to travel, thus raising the total necessary energy to break the specimen. Otherwise, the PV counterpart presented flat layers, meaning a straighter path where the fracture could advance. Another aspect that may have helped reinforce the SV sample is the inertial deposition error caused by the sinusoidal slicing. As Allum et al. [10] noted, there

is a slight delay in the responsiveness of the extruder and the printhead in the direction of movement when printing non-planar, repetitive paths. This phenomenon can be explained by the constant extrusion of filament through the nozzle as it changes direction. When moving and extruding, the nozzle deposits material either toward or against the previous layer in every cycle, causing an asymmetric pattern on the internal layers of the SV and SH specimens that further blocks the natural growth of the crack (Figure 6). These variables are absent in the planar samples, so their layers are cleaner, smoother, and more susceptible to delamination upon stress.

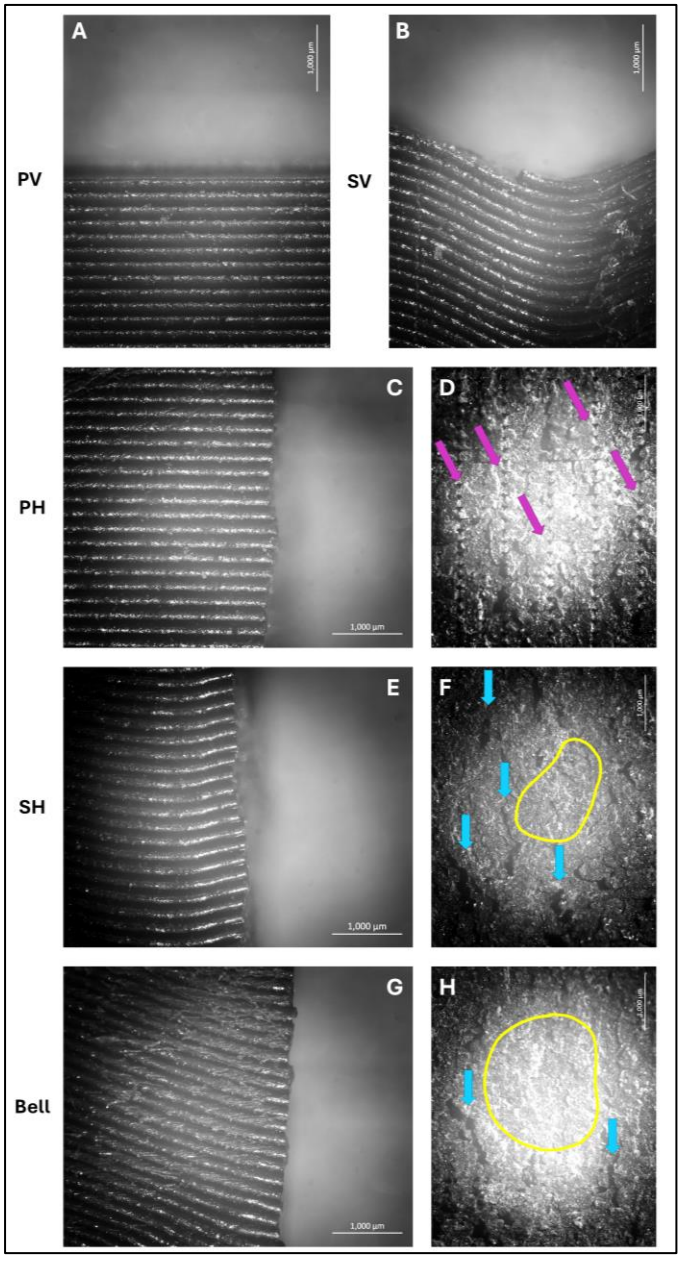

Figure 5. Microscopic analysis of the fracture profiles (A, B, C, E, G) and fracture surfaces (D, F, H). Purple arrows indicate aligned voids, blue arrows point to large or combined voids, and yellow areas exemplify regions with no visible voids

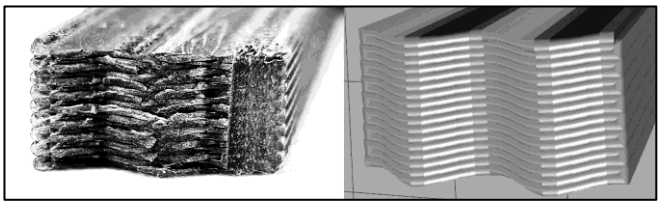

Figure 6. Detailed view of inertial symmetry error caused by non-planar printing (left) vs perfect symmetry on slicing simulation (right)

Horizontal slicing outperformed vertical slicing due to the path of fracture passing through multiple material layers instead of finding gaps between them, as these connections are generally weaker than the material itself. This takeaway agrees with previous publications on impact testing in 3D-printed FFF parts [17-25]. Although there was no significant difference in performance among the horizontal samples, the average impact strength for the Bell and Sinusoidal samples was marginally higher than the planar ones. As for the anisotropy, since there was an increase of resistance in the vertical non-planar slicing, while the horizontal samples had similar results, it is safe to say that the technique helped to bridge the performance gap between vertical and horizontal samples.

All the samples showed brittle behaviour, independent of orientation and slicing technique. This agrees with the impact tests presented in [27] and shows that the non-planar slicing technique increases the bonding between the layers of material. More ductile materials, such as ABS and PETG, could further benefit from this improvement due to their increased capacity to withstand the impact energy before breaking.

V. Conclusion

Non-planar, sinusoidal 3D printing enhanced the mechanical characteristics of FFF parts against impact tests over specific scenarios. Samples printed on weaker orientations and prone to delamination (i.e. vertically printed with layers parallel to the impact) benefited the most from this technique. Even with delamination occurring on the layer boundary of non-planar samples, they still present higher resistance against crack propagation because of the longer and more irregular path the crack must traverse to break the specimen. In the horizontal orientation, the non-planar slicing did not result in a significant difference in the impact resistance of the specimens. Once the interlayer bond in this printing orientation is strong, the crack must rip the individual plastic filament lines apart to advance.

In conclusion, this research provides valuable insights for industries relying on 3D printing to produce tougher and more reliable parts, particularly when specific printing orientations are required. Addressing anisotropy is critical for achieving functional and durable 3D-printed components, and incorporating non-planar slicing options into commercially available slicers could advance efforts to overcome this challenge. For future work, printers with more DoFs can be used to try and correct the deposition errors caused in the non-planar samples, to gauge how much the crack path is disturbed by the curved layers, and how much by the fuzzy and erratic material deposition produced by DoF-limited printers, as well as allowing for more extreme non-planar patterns to achieve better resistance results.

ACKNOWLEDGMENT

This research was supported by the Natural Sciences and Engineering Research Council - Collaborative Research and Training Experience (NSERC - CREATE) (2020-543378)

REFERENCES

[1] S. Ahn, M. Montero, D. Odell, S. Roundy, and P. K. Wright, "Anisotropic material properties of fused deposition modeling ABS," Rapid Prototyping Journal, vol. 8, no. 4, pp. 248–257, Oct. 2002, doi: https://doi.org/10.1108/13552540210441166.

[2] D. Chakraborty, B. Aneesh Reddy, and A. Roy Choudhury, "Extruder path generation for Curved Layer Fused Deposition Modeling," Computer-Aided Design, vol. 40, no. 2, pp. 235–243, Feb. 2008, doi: https://doi.org/10.1016/j.cad.2007.10.014.

[3] P. Tang et al., "A review of multi-axis additive manufacturing: Potential, opportunity and challenge," Additive Manufacturing, vol. 83, p. 104075, Mar. 2024, doi: https://doi.org/10.1016/j.addma.2024.104075.

[4] Y. Yao, L. Cheng, and Z. Li, "A comparative review of multi-axis 3D printing," Journal of manufacturing processes, vol. 120, pp. 1002–1022, Jun. 2024, doi: https://doi.org/10.1016/j.jmapro.2024.04.084.

[5] G. Fang, S. Zhong, Z. Zhong, T. Zhang, X. Chen, and C. Wang, "Reinforced FDM: Multi-Axis Filament Alignment with Controlled Anisotropic Strength," ACM Transactions on Graphics (TOG), vol. 39, no. 6, 2020, doi: https://doi.org/10.1145/3414685.3417834.

[6] K.-M. .M. Tam, K. T. Mueller, J. R. Coleman, and N. W. Fine, "Stress Line Additive Manufacturing (SLAM) for 2.5-D Shells," Journal of the International Association for Shell and Spatial Structures, vol. 57, no. 4, pp. 249–259, Dec. 2016, doi: https://doi.org/10.20898/j.iass.2016.190.856.

[7] S. Singamneni, A. Roychoudhury, O. Diegel, and B. Huang, "Modeling and evaluation of curved layer fused deposition," Journal of Materials Processing Technology, vol. 212, no. 1, pp. 27–35, Jan. 2012, doi: https://doi.org/10.1016/j.jmatprotec.2011.08.001.

[8] A. T. Alsharhan, T. Centea, and S. K. Gupta, "Enhancing Mechanical Properties of Thin-Walled Structures Using Non-Planar Extrusion Based Additive Manufacturing," Volume 2: Additive Manufacturing; Materials, Jun. 2017, doi: https://doi.org/10.1115/msec2017-2978.

[9] N. Fry, R. M. Richardson, and J. H. Boyle, "Robotic additive manufacturing system for dynamic build orientations," Rapid Prototyping Journal, vol. 26, no. 4, pp. 659–667, Jan. 2020, doi: https://doi.org/10.1108/rpj-09-2019-0243.

[10] J. Allum, J. Kitzinger, Y. Li, V. V. Silberschmidt, and A. Gleadall, "ZigZagZ: Improving mechanical performance in extrusion additive manufacturing by nonplanar toolpaths," Additive Manufacturing, vol. 38, p. 101715, Feb. 2021, doi: https://doi.org/10.1016/j.addma.2020.101715.

[11] R. Edwards and L. Clemon, "Influencing the Mechanical Properties of Fused Filament Fabrication Parts by Non-Planar Material Extrusion," in Volume 2A: Advanced Manufacturing, American Society of Mechanical Engineers, Nov. 2021. doi: https://doi.org/10.1115/imece2021-70144.

[12] Y. Li, D. He, S. Yuan, K. Tang, and J. Zhu, "Vector field-based curved layer slicing and path planning for multi-axis printing," Robotics and Computer-Integrated Manufacturing, vol. 77, p. 102362, Oct. 2022, doi: https://doi.org/10.1016/j.rcim.2022.102362.

[13] J. B. Khurana, T. W. Simpson, and M. Frecker, "Structurally Intelligent 3D Layer Generation for Active-Z Printing," in Proceedings of the 29th Annual International Solid Freeform Fabrication Symposium, Jan. 2018. doi: https://doi.org/10.26153/tsw/17234.

[14] A. Gleadall, "FullControl GCode Designer - open-source software for unconstrained design in additive manufacturing," Additive Manufacturing, vol. 46, p. 102109, Jun. 2021, doi: https://doi.org/10.1016/j.addma.2021.102109.

[15] Y. Kayali, M. Ding, S. Hamdallah, S. Qi, R. Bibb, and A. Gleadall, "Effect of printing parameters on microscale geometry for 3D printed lattice structures," Materials Today: Proceedings, vol. 70, Sep. 2022, doi: https://doi.org/10.1016/j.matpr.2022.08.487.

[16] ASTM International, "Test Method for Determining the Charpy Impact Resistance of Notched Specimens of Plastics," Apr. 2018, doi: https://doi.org/10.1520/d6110-18.

[17] Md. Q. Tanveer, A. Haleem, and M. Suhaib, "Effect of variable infill density on mechanical behaviour of 3-D printed PLA specimen: an experimental investigation," SN Applied Sciences, vol. 1, no. 12, Nov. 2019, doi: https://doi.org/10.1007/s42452-019-1744-1.

[18] I. Fekete, F. Ronkay, and L. Lendvai, "Highly toughened blends of poly(lactic acid) (PLA) and natural rubber (NR) for FDM-based 3D printing applications: The effect of composition and infill pattern," Polymer Testing, vol. 99, p. 107205, Jul. 2021, doi: https://doi.org/10.1016/j.polymertesting.2021.107205.

[19] J. Andrzejewski, M. Markowski, and M. Barczewski, "The Use of Nanoscale Montmorillonite (MMT) as Reinforcement for Polylactide Acid (PLA) Prepared by Fused Deposition Modeling (FDM)—Comparative Study with Biocarbon and Talc Fillers," Materials, vol. 15, no. 15, p. 5205, Jan. 2022, doi: https://doi.org/10.3390/ma15155205.

[20] Y. P. Shaik, J. Schuster, and N. K. Naidu, "High-Pressure FDM 3D Printing in Nitrogen [Inert Gas] and Improved Mechanical Performance of Printed Components," Journal of Composites Science, vol. 7, no. 4, p. 153, Apr. 2023, doi: https://doi.org/10.3390/jcs7040153.

[21] L. P. Muthe, K. Pickering, and C. Gauss, "Polylactide Composites Reinforced with Pre-Impregnated Natural Fibre and Continuous Cellulose Yarns for 3D Printing Applications," Materials, vol. 17, no. 22, pp. 5554–5554, Nov. 2024, doi: https://doi.org/10.3390/ma17225554.

[22] J. Shang et al., "Impact resistance of biomimetic gradient sinusoidal composites by 3D printing: Tunable structural stiffness and damage tolerance," Composites Part B Engineering, vol. 291, pp. 112016–112016, Nov. 2024, doi: https://doi.org/10.1016/j.compositesb.2024.112016.

[23] G. Murariu, Matei Marin-Corciu, and Sergiu-Valentin Galaţanu, "Evaluation of the layering adhesion between PLA and TPE materials," IOP Conference Series Materials Science and Engineering, vol. 1319, no. 1, pp. 012036–012036, Oct. 2024, doi: https://doi.org/10.1088/1757-899x/1319/1/012036.

[24] M. Głowacki, K. Skórczewska, K. Lewandowski, A. Mazurkiewicz, and P. Szewczykowski, "Evaluation of the Effect of Mineral Oil Exposure on Changes in the Structure and Mechanical Properties of Polymer Parts Produced by Additive Manufacturing Techniques," Materials, vol. 17, no. 15, pp. 3680–3680, Jul. 2024, doi: https://doi.org/10.3390/ma17153680.

[25] M. Głowacki, K. Skórczewska, K. Lewandowski, P. Szewczykowski, and A. Mazurkiewicz, "Effect of Shock-Variable Environmental Temperature and Humidity Conditions on 3D-Printed Polymers for Tensile Properties," Polymers, vol. 16, no. 1, pp. 1–1, Dec. 2023, doi: https://doi.org/10.3390/polym16010001.

[26] A. E. Musteaţă, C. Pirvu, L. Deleanu, and C. Georgescu, "Simulation of Charpy test for different impact velocities," IOP Conference Series: Materials Science and Engineering, vol. 514, no. 1, p. 012011, May 2019, doi: https://doi.org/10.1088/1757-899x/514/1/012011.

[27] T. Tezel, M. Ozenc, and V. Kovan, "Impact properties of 3D-printed engineering polymers," Materials Today Communications, vol. 26. Elsevier BV, p. 102161, Mar. 2021. doi: 10.1016/j.mtcomm.2021.102161.